Catal Lett (2009) 129:287–292
DOI 10.1007/s10562-008-9818-5

On the Role of Aging, Washing, and Drying in the Synthesis of Polycrystalline Zinc Oxide by Precipitation: Combining Fast Continuous Mixing, Spray Drying and Freeze Drying to Unravel the Solid-State Transformations of the Precipitate

Stefan Kaluza · Martin Muhler

Received: 21 August 2008 / Accepted: 5 December 2008 / Published online: 23 December 2008

Abstract The continuous precipitation of zinc carbonates using aqueous solutions of zinc nitrate and sodium carbonate was quenched within a few seconds by combining a micromixer with a bench-top spray dryer. In this way, it was possible to monitor the slow phase transformation of the initially formed sodium zinc carbonate into zinc hydroxy carbonate during subsequent washing and drying. An increased stirring rate applied during washing was found to accelerate this phase transformation, thus influencing the specific surface areas and pore size distributions of the ZnO powder materials finally obtained after calcination.

Keywords ZnO · Continuous precipitation · Micromixing · Spray drying · Freeze drying

1 Introduction

Precipitation plays an important role in the field of bulk catalyst preparation [1]. Due to its high degree of flexibility, the generation of homogeneous component distributions and the possibility to create pure materials, it is one of the most frequently applied synthetic methods. Polycrystalline zinc oxide can be prepared by the precipitation of zinc salts with alkali carbonates or hydroxides followed by a controlled calcination process [2]. ZnO is catalytically active in hydrogenation reactions [3], or it is used as catalyst support [4, 5]. Other catalysts of industrial importance prepared by precipitation methods are the catalysts for Fischer–Tropsch synthesis [6], the V/P/O catalyst for the oxidation of *n*-butane to maleic anhydride [7, 8], and the Cu/ZnO catalyst for methanol synthesis [4, 5]. In the latter case, Bems et al. [9] showed that the properties and performance of the final catalyst are strongly influenced by a large set of experimental parameters applied during the precipitation process. They investigated the particle formation of binary catalyst precursors by varying the pH, the Cu–Zn ratio, and the aging time, and observed that the system is extremely sensitive to small changes of the synthesis conditions. Additionally, further parameters such as temperature, concentration, solvent, flow rates and stirrer speed have to be considered [1]. This huge set of parameters for one specific precipitation process requires an elaborate optimization.

The degree of supersaturation that is created by bringing the corresponding solutions into contact is essential for the particle formation [10]. During a conventional precipitation in a batch reactor local supersaturation is created when a droplet of one solution hits the other solution. Due to intensive stirring the system is homogenized on a short timescale, and the local supersaturation vanishes. In contrast, a continuous precipitation leads to a constant supersaturation level and therefore to a more homogenous nucleation [11].

Recently, a microscale mixing tee was used as a continuous flow reactor for the precipitation of zinc nitrate with sodium carbonate [12]. This mixing tee provides laminar flow in and out of the mixing zone, while the mixing occurs under turbulent conditions due to the special geometry of the device. The volume of the mixing zone is less than 0.03 mL resulting in very fast mixing and an estimated residence time of the precipitate of less than 0.3 s in the turbulent region of the mixing tee. These conditions influence the particle size of the final zinc oxide and its specific properties [13]. The mixing tee was directly connected to the two-fluid nozzle of a bench-top spray dryer.

S. Kaluza · M. Muhler (✉)
Laboratory of Industrial Chemistry, Ruhr-University Bochum, Universitätsstr. 150, 44780 Bochum, Germany
e-mail: muhler@techem.rub.de

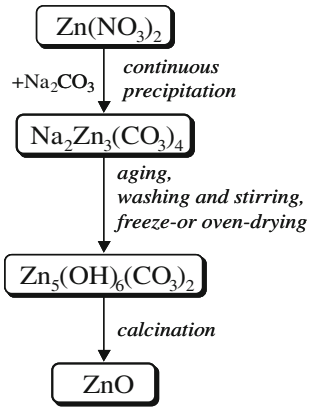

Fig. 1 Experimental strategy to synthesize nanoscale zinc oxide via continuous precipitation combined with rapid spray drying, followed by washing, drying and calcination

With this combined set-up the precipitation reaction was quenched immediately, and the initially formed precursor was investigated by powder X-ray diffraction (XRD), N_2 physisorption, scanning electron microscopy (SEM), and atomic absorption spectroscopy (AAS). The immediate quenching of the precipitation of zinc nitrate with sodium carbonate led to the formation of the kinetically favored precursor. This instantly formed phase was identified as the sodium zinc carbonate $Na_2Zn_3(CO_3)_4$ [14]. When this phase was then exposed to water during the washing step to remove the byproduct sodium nitrate, a structural rearrangement of the system took place, and the thermodynamically more favored zinc hydroxy carbonate $Zn_5(OH)_6(CO_3)_2$ was formed [15]. Usually, zinc hydroxy carbonate is referred to as the precipitation product achieved by the conventionally precipitation in a batch reactor followed by several hours of aging [9, 16].

In the present contribution, the unit operations applied during the post-precipitation processes, i.e., aging, washing and drying, were studied in detail (Fig. 1). The use of a freeze dryer offered the possibility to separate the changes during washing from those during the subsequent drying in the drying oven. Therefore, it was possible to investigate the transformations occurring during washing separately without further thermal treatment of the precursor, and a strong influence of the stirrer speed on the rate of the phase transition was detected.

2 Experimental

2.1 Preparation

The zinc oxide precursor was prepared by a continuous precipitation of aqueous zinc nitrate solution ($c = 0.10$ mol L^{-1}) with aqueous sodium carbonate solution ($c = 0.12$ mol L^{-1}) using a mixing tee (VICI) as microreactor. The chemicals were obtained from Aldrich and used as received. The mixing tee was directly connected to a bench-top spray dryer (BÜCHI) or separated from the latter by a continuous aging device. This device consisted of a 7 m silicone tubing with an inner diameter of 0.5 cm and provided a residence time of the precipitate of 18 min before the spray drying process. All spray-dried samples were washed three times for 5 min with 20 mL of distilled water stirring with a defined stirrer speed inside a glass frit (porosity 5, pore size 1.0–1.6 μm). After filtration, the washed precursor was oven-dried for 20 h at 120 °C or freeze-dried for 20 h at −50 °C and 0.1 mbar. The precursors were calcined for 3 h at 280 °C under synthetic air flow (20% O_2 in N_2) using a bench-top rotary kiln.

2.2 Characterization

Powder XRD patterns were recorded in the 2θ range from 5 to 80° (step width of 0.03°) using a Panalytical MPD diffractometer, equipped with a copper tube, 0.5° divergent and antiscatter slit, a 0.2 mm high receiving slit, incident and diffracted beam 0.04 rad soller slits and a secondary graphite monochromator. Powder diffraction files (PDF) from the international centre of diffraction data (ICDD) combined with the X′Pert line software (Panalytical, Almeno) were used for qualitative phase analysis. Lanthanum hexaboride NIST-SRM 660a was used to correct for instrumental line broadening. Static nitrogen physisorption experiments were performed in a modified Autosorb 1C set-up (Quantachrome). All samples were pretreated at 200 °C for 2 h. Data were analysed according to the BET equation, assuming that the area covered by a nitrogen molecule equals 0.162 nm^2. The pore size distribution was obtained using the BJH method. SEM measurements of the powder materials were performed with a high resolution thermally aided field SEM (Zeiss, LEO 1530 Gemini). AAS measurements were performed using a Thermo electron spectrometer (M-series).

3 Results and Discussion

3.1 The Role of Aging

The phase transition of the sodium zinc carbonate into the zinc hydroxy carbonate plays an important role during the preparation process and is achieved by exposing the spray-dried precursor to water again. To investigate this effect in more detail, a continuous ageing device was added to the mixing tee/spray dryer set-up. This residence time module consisted of a silicone tubing of defined length and diameter that was applied between the mixing tee and the nozzle of the spray dryer. Consequently, the precipitate was in

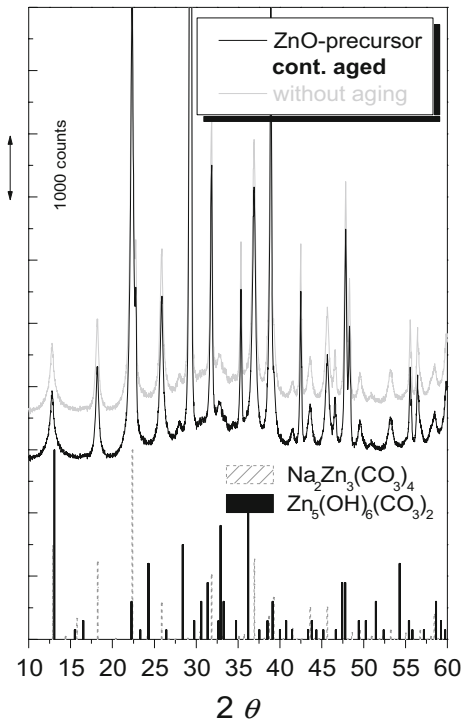

Fig. 2 XRD pattern of the spray-dried precursor that was aged for 18 min in the residence time module. The pattern of the immediately spray-dried precursor (*light gray line*) as well as the data of the powder diffraction files of $Na_2Zn_3(CO_3)_4$ (86-0607) and $Zn_5(OH)_6(CO_3)_2$ (19-1458) are included for comparison

contact with its mother liquid, usually referred to as ageing, for additional 18 min before it was spray-dried. The residence time of 18 min was chosen in the range of the exposure time during the washing process. The flow through the module in this case was laminar due to the chosen set-up conditions. Figure 2 shows the XRD pattern of the resulting spray-dried precursor. The comparison of the two patterns illustrates that there is no difference in phase composition between the immediately spray-dried precursor and the continuously aged precursor. In both cases the sodium zinc carbonate is—in addition to sodium nitrate—the predominant phase. Thus, aging in the residence time module under laminar flow conditions does not lead to a phase transition.

3.2 The Role of the Washing and Drying Steps

As the flow through the residence time module was laminar, intensive mass transport during the continuous aging of the precipitate did not take place. Moreover, the 18 min of aging took place at room temperature. In contrast to this method, the washing and drying steps provide fast mass transport due to the intensive stirring during washing as well as a thermal treatment of the moist sample during drying in the oven. Thus, the phase transition of the sodium zinc carbonate into the zinc hydroxy carbonate seems to be an activated process that requires additional energy.

To explore whether the intensive stirring or the thermal treatment is responsible for the phase transition, the washing and the drying step have to be investigated separately. Therefore, one part of a freshly washed precursor was dried using a freeze dryer. The advantage of this method is the possibility to investigate the sample by means of powder XRD without using temperatures higher than room temperature. The other part of the same freshly washed sample was dried as usual at 120 °C in a drying oven, so that the influence of stirring can be studied unimpaired by subsequent drying (Fig. 3).

The XRD pattern of the freeze-dried sample shows the sharp and intensive reflections of the sodium zinc carbonate as well as the broader reflections of the zinc hydroxy carbonate, while the washed and oven-dried sample exclusively consists of the latter phase. These results indicate that the phase transition already starts during washing—but does not proceed completely—and continues during drying. This continuation of the phase transition during drying occurs presumably due to the residual moisture of the sample when it is placed inside the drying oven directly after washing [17, 18]. It is not just a thermal decomposition of the residual sodium zinc carbonate,

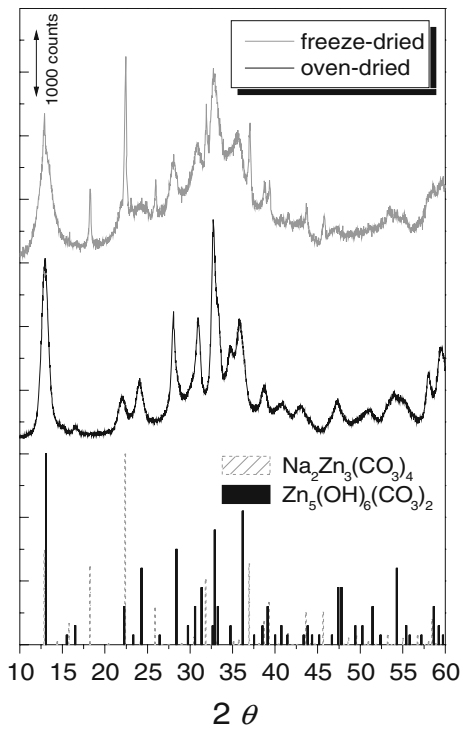

Fig. 3 XRD patterns of the immediately spray-dried and washed precursor that was divided into two parts and then oven-dried or freeze-dried, respectively. The data of the powder diffraction files of $Na_2Zn_3(CO_3)_4$ (86-0607) and $Zn_5(OH)_6(CO_3)_2$ (19-1458) are included for comparison

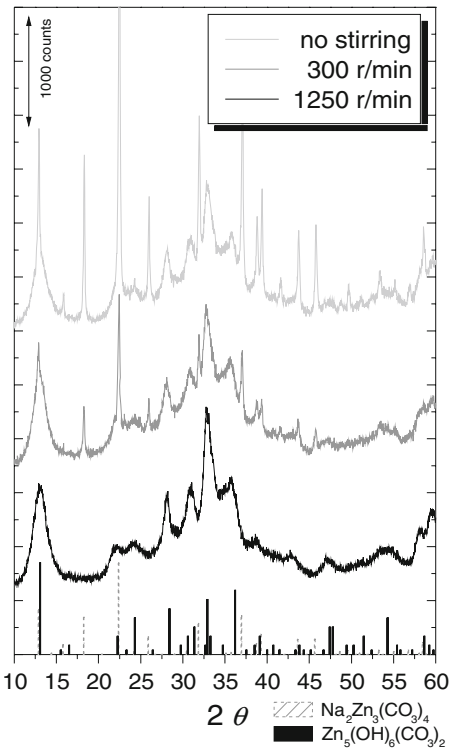

Fig. 4 XRD patterns of the spray-dried precursor washed without stirring (*light gray, top*), with 300 r/min (*gray, middle*), and 1,250 r/min (*black, bottom*). All samples were freeze-dried afterwards. The data of the powder diffraction files of $Na_2Zn_3(CO_3)_4$ (86-0607) and $Zn_5(OH)_6(CO_3)_2$ (19-1458) are included for comparison

because otherwise the reflections of the decomposition products—zinc oxide and sodium carbonate—would have to be present. Furthermore, when the freeze-dried sample was treated at 120 °C for 20 h no changes in the resulting XRD pattern were observed, further supporting this hypothesis.

3.3 The Role of Stirring

As the continuous aging as well as washing both occur at room temperature, the increased mass transport due to intensive stirring has to be one of the reasons for the observed phase transition from $Na_2Zn_3(CO_3)_4$ to $Zn_5(OH)_6(CO_3)_2$. Another factor is the beneficial sodium gradient, which is present during washing with distilled water. To prove the assumption that the rate of the phase transition is a function of the applied stirrer speed, three spray-dried samples were washed without stirring, with 300 r/min and with 1,250 r/min, respectively, by keeping all other parameters constant. Figure 4 shows the three resulting XRD patterns of the subsequently freeze-dried precursors.

The XRD results clearly show that the rate of the phase transition during washing is influenced by the stirrer speed. Sodium zinc carbonate is still the predominant phase in the sample that was not stirred at all, while the sample with the highest stirrer speed consists only of zinc hydroxy carbonate indicating a complete phase transition.

Additionally, intensive stirring leads to a breaking up of previously formed agglomerates (Fig. 5). In the present case, spherical agglomerates were formed due to the spray-drying process. Fragmenting these spheres leads to an increased mass transfer and also to a rearrangement into less regularly formed smaller agglomerates after subsequent drying.

For further investigations the three freeze-dried samples were calcined, and the resulting zinc oxides were characterized (Table 1). The XRD patterns of the three samples all consist of phase-pure zinc oxide (wurtzite), and the reflections do not differ in width and intensity. Moreover, based on the Debye-Scherrer equation all samples exhibit a mean crystallite size of about 7 nm. However, the calcined precursors show significant differences concerning the specific surface areas using the BET method (Table 1). The reason for this variation in surface area is caused by different pore structures of the samples. The pore size distributions derived by the BJH method reveal bimodal distribution profiles for each sample, with two maxima at about 4 and 30 nm pore diameter (Fig. 6). The relative amounts of smaller and larger pores differ and are correlated with the BET surface areas, with the sample with the

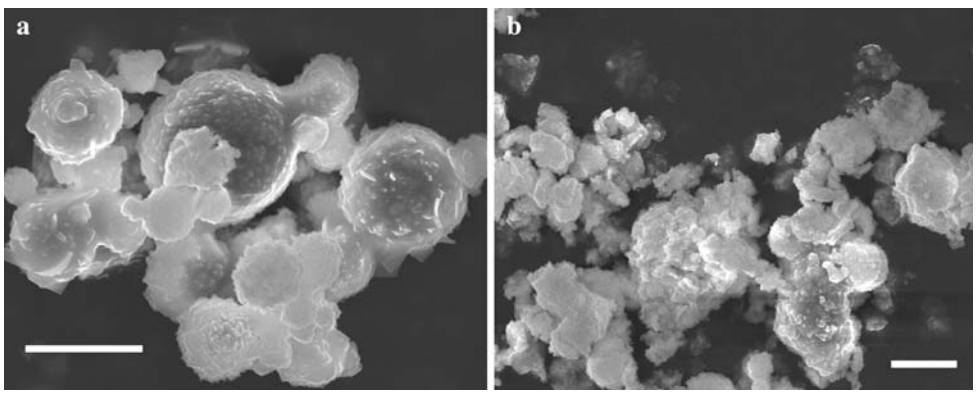

Fig. 5 SEM images of **a** the continuously precipitated and spray-dried ZnO-precursor and **b** the subsequently washed and oven-dried precursor. Stirring leads to a fragmentation of the previously formed precursor spheres. *Scale bars* 2 μm

Table 1 Residual amount of sodium in the zinc oxide samples (AAS) as a function of stirrer speed, mean crystallite size estimated by the Debye-Scherrer equation, and the according specific surface areas (BET)

Stirrer speed	No stirring	300 r/min	1,250 r/min
Residual Na(wt%)	5.3	2.2	1.2
Mean crystallite size(nm)	7.1	7.0	7.2
BET surface area/(m^2 g^{-1})	58.8	88.1	76.1

highest BET surface area exhibiting the largest amount of smaller pores. As all three samples were calcined in exactly the same way, those structural differences can only be due to the difference in phase composition before the calcination caused by the variation of the stirrer speed.

All samples contain a small amount of residual sodium in the final zinc oxide (Table 1). However, this residual sodium content does not result from an incomplete removal of ionic nitrate by washing. Sodium nitrate has a very high solubility in water even at room temperature [19]. Electrical conductivity measurements as preliminary tests revealed a complete dissolution and removal of solid sodium nitrate under the applied washing conditions. Moreover, when the spray-dried sample was calcined first to decompose the sodium zinc carbonate into zinc oxide and water-soluble sodium carbonate, and was then washed afterwards, no residual amount of sodium was detected by AAS. Therefore, the residual sodium content of the samples is caused by the incomplete phase transition of the sodium zinc carbonate into the zinc hydroxy carbonate before the calcination. As shown in Table 1, the amount of residual sodium correlates well with the stirrer speed, which leads to different amounts of sodium zinc carbonate in the washed sample. It is still an open question which kind of residual chemical sodium species is present in the calcined sample. The XRD patterns provide no hints on any other crystalline phases than zinc oxide. Therefore, additional characterization methods such as IR and Raman spectroscopy are used in ongoing studies to clarify this question.

4 Conclusions

The set-up combining continuous precipitation in a microreactor with an immediate quenching of the reaction by a rapid spray-drying process provided a new promising method to investigate precipitation reactions in more detail. Structural transformations were quenched, and a detailed analysis of the occurring processes during the first few seconds of the precipitation became feasible.

Moreover, the additional application of freeze drying offered the opportunity to separate the influence of the washing step from that of the drying step by allowing to characterize the washed precursors without any further thermal treatment.

Sodium zinc carbonate was identified as the kinetically controlled first precipitation product from zinc nitrate with

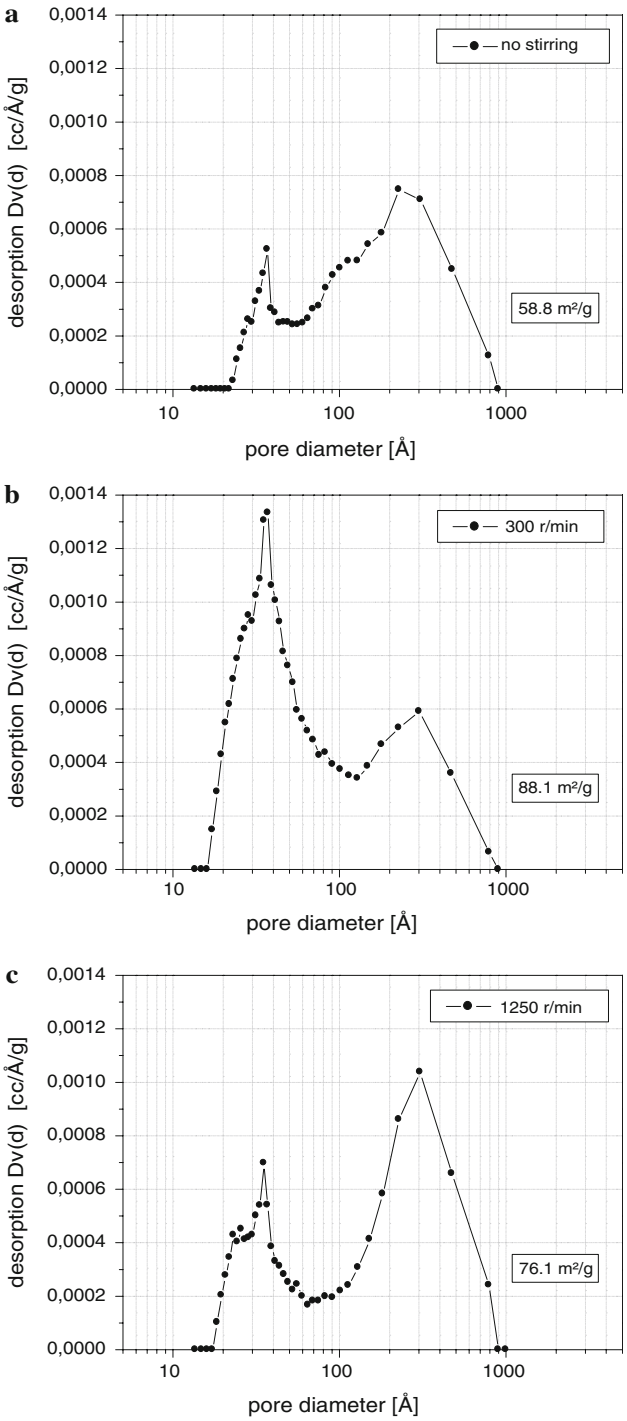

Fig. 6 XRD patterns of the calcined zinc oxide precursors washed with different stirrer speeds: without stirring, 300, and 1,250 r/min, respectively (*top*) and the according pore size distributions including the specific surface areas of each sample (*bottom*)

sodium carbonate. Washing led to a rearrangement of the instantly formed sodium zinc carbonate to the thermodynamically more stable precursor zinc hydroxy carbonate. This phase transition turned out to be an activated process, which was accelerated by intensive stirring.

Consequently, during catalyst synthesis attention should not only be paid to the precipitation, but also to the post-precipitation steps, as they strongly influence the properties of the final calcined material.

Acknowledgments The authors gratefully acknowledge fruitful discussions with Malte Behrens and Robert Schlögl, and the financial support by the BMBF (Bundesministerium für Bildung und Forschung) within the scope of the project 01RI05028 "Entwicklung von Methanolsynthesekatalysatoren als Basis für nachhaltige Ressourcennutzung".

References

1. Schüth F, Unger K (1997) In: Ertl G, Knözinger H, Weitkamp J (eds) Handbook of heterogeneous catalysis, vol 1. Wiley-VCH, Weinheim (chap. 2.1.3)
2. Pfaff G (2005) In: Dittmeyer R, Keim W, Kreysa G, Oberholz A (eds) Chem Tech, vol 7. Wiley-VCH, Weinheim (chap. 3)
3. Tabatabaei J, Sakakini BH, Waugh KC (2006) Catal Lett 110:77
4. Hansen PL, Wagner JB, Helveg S, Rostrup-Nielsen JR, Clausen BS, Topsøe H (2002) Science 295:2053
5. Wilmer H, Hinrichsen O (2002) Catal Lett 82:117
6. Dyer PN, Nordquist AF, Pierantozzi R (1986) Air Products and Chemicals Inc. US Patent 4 624 942
7. Burnett JC, Keppel RA, Robinson WD (1987) Catal Today 1:537
8. Centi G (1993) Catal Today 16:5
9. Bems B, Schur M, Dassenoy A, Junkes H, Herein D, Schlögl R (2003) Chem Eur J 9:2039
10. Kucher M, Kind M (2007) Chem Ing Tech 79:266
11. Kucher M, Babic D, Kind M (2006) Chem Eng Process 45:900
12. Kaluza S, Schröter MK, Naumann d'Alnoncourt R, Reinecke T, Muhler M (2008) Adv Funct Mater 18:3670
13. Schur M, Bems B, Dassenoy A, Kassatkine I, Urban J, Wilmer H, Hinrichsen O, Muhler M, Schlögl R (2003) Angew Chem Int Ed 42:3815
14. Gier TE, Bu X, Wang SL, Stucky GD (1996) J Am Chem Soc 118:3039
15. Fujita SI, Satriyo AM, Shen GC, Takezawa N (1995) Catal Lett 34:85
16. Skapin SD, Drazic G, Orel ZC (2007) Mater Lett 61:2783
17. Chouillet C, Villain F, Kermarec M, Lauron-Pernot H, Louis C (2003) J Phys Chem B 107:3565
18. Catillon-Mucherie S, Ammari F, Krafft JM, Lauron-Pernot H, Touroude R, Louis C (2007) J Phys Chem C 111:11619
19. RC C (1993) In: Lide DR (ed) Handbook of Chemistry and Physics, vol 74. CRC Press, Boca Raton, Florida